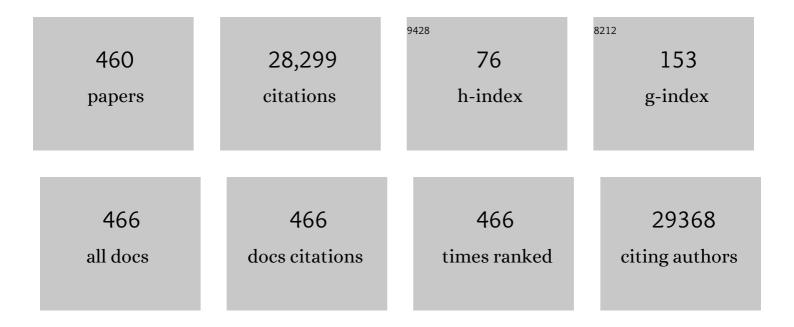
## Martin Leach

List of Publications by Year in descending order

Source: https://exaly.com/author-pdf/2757013/publications.pdf Version: 2024-02-01



#	Article	IF	CITATIONS
1	A novel roadmap connecting the 1H-MRS total choline resonance to all hallmarks of cancer following targeted therapy. European Radiology Experimental, 2021, 5, 5.	1.7	5
2	Quantifying MRI <i>T</i> <sub>1</sub> relaxation in flowing blood: implications for arterial input function measurement in DCE-MRI. British Journal of Radiology, 2021, 94, 20191004.	1.0	2
3	Early response to chemotherapy in malignant pleural mesothelioma assessed using diffusion-weighted MRI: Initial observations. JTO Clinical and Research Reports, 2021, 2, 100253.	0.6	Ο
4	DCE-MRI is more sensitive than IVIM-DWI for assessing anti-angiogenic treatment-induced changes in colorectal liver metastases. Cancer Imaging, 2021, 21, 67.	1.2	4
5	<i>De novo</i> phosphatidylcholine synthesis is required for autophagosome membrane formation and maintenance during autophagy. Autophagy, 2020, 16, 1044-1060.	4.3	67
6	Increased inflammatory lipid metabolism and anaplerotic mitochondrial activation follow acquired resistance to vemurafenib in BRAF-mutant melanoma cells. British Journal of Cancer, 2020, 122, 72-81.	2.9	21
7	Psychosocial effects of whole-body MRI screening in adult high-risk pathogenic <i>TP53</i> mutation carriers: a case-controlled study (SIGNIFY). Journal of Medical Genetics, 2020, 57, 226-236.	1.5	15
8	Noise-Corrected, Exponentially Weighted, Diffusion-Weighted MRI (niceDWI) Improves Image Signal Uniformity in Whole-Body Imaging of Metastatic Prostate Cancer. Frontiers in Oncology, 2020, 10, 704.	1.3	10
9	Monocarboxylate transporter 1 blockade with AZD3965 inhibits lipid biosynthesis and increases tumour immune cell infiltration. British Journal of Cancer, 2020, 122, 895-903.	2.9	74
10	Supervised Machine-Learning Enables Segmentation and Evaluation of Heterogeneous Post-treatment Changes in Multi-Parametric MRI of Soft-Tissue Sarcoma. Frontiers in Oncology, 2019, 9, 941.	1.3	22
11	Utility of Multi-Parametric Quantitative Magnetic Resonance Imaging for Characterization and Radiotherapy Response Assessment in Soft-Tissue Sarcomas and Correlation With Histopathology. Frontiers in Oncology, 2019, 9, 280.	1.3	24
12	Synthetic 4D-CT of the thorax for treatment plan adaptation on MR-guided radiotherapy systems. Physics in Medicine and Biology, 2019, 64, 115005.	1.6	10
13	Post-radiotherapy apparent diffusion coefficient (ADC) in children and young adults with high-grade gliomas and diffuse intrinsic pontine gliomas. Pediatric Hematology and Oncology, 2019, 36, 103-112.	0.3	7
14	Methodological consensus on clinical proton MRS of the brain: Review and recommendations. Magnetic Resonance in Medicine, 2019, 82, 527-550.	1.9	280
15	Growth Trajectories, Breast Size, and Breast-Tissue Composition in a British Prebirth Cohort of Young Women. American Journal of Epidemiology, 2018, 187, 1259-1268.	1.6	6
16	Characterisation of fibrosis in chemically-induced rat mammary carcinomas using multi-modal endogenous contrast MRI on a 1.5T clinical platform. European Radiology, 2018, 28, 1642-1653.	2.3	3
17	Quantitative evaluation of contrast agent uptake in standard fatâ€suppressed dynamic contrastâ€enhanced MRI examinations of the breast. Medical Physics, 2018, 45, 287-296.	1.6	7
18	Changes in multimodality functional imaging parameters early during chemoradiation predict treatment response in patients with locally advanced head and neck cancer. European Journal of Nuclear Medicine and Molecular Imaging, 2018, 45, 759-767.	3.3	35

#	Article	IF	CITATIONS
19	MRI-based Assessment of 3D Intrafractional Motion of Head and Neck Cancer for RadiationÂTherapy. International Journal of Radiation Oncology Biology Physics, 2018, 100, 306-316.	0.4	28
20	Circulating Growth and Sex Hormone Levels and Breast Tissue Composition in Young Nulliparous Women. Cancer Epidemiology Biomarkers and Prevention, 2018, 27, 1500-1508.	1.1	4
21	Reproducibility of the lung anatomy under active breathing coordinator control: Dosimetric consequences for scanned proton treatments. Medical Physics, 2018, 45, 5525-5534.	1.6	8
22	Metabolic biomarkers of response to the AKT inhibitor MK-2206 in pre-clinical models of human colorectal and prostate carcinoma. British Journal of Cancer, 2018, 119, 1118-1128.	2.9	13
23	PO-0959: Dosimetric Evaluation of Midposition Pseudo-CT for MR-only Lung Radiotherapy Treatment planning. Radiotherapy and Oncology, 2018, 127, S526-S527.	0.3	2
24	Prospective multicentre evaluation and refinement of an analysis tool for magnetic resonance spectroscopy of childhood cerebellar tumours. Pediatric Radiology, 2018, 48, 1630-1641.	1.1	7
25	Microstructure Characterization of Bone Metastases from Prostate Cancer with Diffusion MRI: Preliminary Findings. Frontiers in Oncology, 2018, 8, 26.	1.3	9
26	Evaluating Imaging Biomarkers of Acquired Resistance to Targeted EGFR Therapy in Xenograft Models of Human Head and Neck Squamous Cell Carcinoma. Frontiers in Oncology, 2018, 8, 271.	1.3	9
27	Super-resolution T2-weighted 4D MRI for image guided radiotherapy. Radiotherapy and Oncology, 2018, 129, 486-493.	0.3	16
28	Abstract 4108: Longitudinal diffusion-weighted MRI assessment of NRAS mutant melanoma response to dual RAF-MEK inhibition reveals differences associated with collagen deposition. , 2018, , .		0
29	Repeatability of derived parameters from histograms following non-Gaussian diffusion modelling of diffusion-weighted imaging in a paediatric oncological cohort. European Radiology, 2017, 27, 345-353.	2.3	40
30	A computerized volumetric segmentation method applicable to multi-centre MRI data to support computer-aided breast tissue analysis, density assessment and lesion localization. Medical and Biological Engineering and Computing, 2017, 55, 57-68.	1.6	21
31	Baseline results from the UK SIGNIFY study: a whole-body MRI screening study in TP53 mutation carriers and matched controls. Familial Cancer, 2017, 16, 433-440.	0.9	52
32	Lung volume reproducibility under ABC control and self-sustained breath-holding. Journal of Applied Clinical Medical Physics, 2017, 18, 154-162.	0.8	15
33	Breast MRI segmentation for density estimation: Do different methods give the same results and how much do differences matter?. Medical Physics, 2017, 44, 4573-4592.	1.6	23
34	A generalized framework unifying image registration and respiratory motion models and incorporating image reconstruction, for partial image data or full images. Physics in Medicine and Biology, 2017, 62, 4273-4292.	1.6	43
35	P2.05-042 Development of Thoracic Magnetic Resonance Imaging (MRI) for Radiotherapy Planning. Journal of Thoracic Oncology, 2017, 12, S1057.	0.5	1
36	Noninvasive Imaging of Cycling Hypoxia in Head and Neck Cancer Using Intrinsic Susceptibility MRI. Clinical Cancer Research, 2017, 23, 4233-4241.	3.2	33

#	Article	IF	CITATIONS
37	Extracranial Soft-Tissue Tumors: Repeatability of Apparent Diffusion Coefficient Estimates from Diffusion-weighted MR Imaging. Radiology, 2017, 284, 88-99.	3.6	45
38	Accuracy of screening women at familial risk of breast cancer without a known gene mutation: Individual patient data meta-analysis. European Journal of Cancer, 2017, 85, 31-38.	1.3	32
39	MCT1 Inhibitor AZD3965 Increases Mitochondrial Metabolism, Facilitating Combination Therapy and Noninvasive Magnetic Resonance Spectroscopy. Cancer Research, 2017, 77, 5913-5924.	0.4	96
40	Detecting human melanoma cell re-differentiation following BRAF or heat shock protein 90 inhibition using photoacoustic and magnetic resonance imaging. Scientific Reports, 2017, 7, 8215.	1.6	10
41	OC-0303: Evaluation of lung anatomy vs. lung volume reproducibility for scanned proton treatments under ABC Radiotherapy and Oncology, 2017, 123, S156-S157.	0.3	0
42	Magnetic Resonance Imaging–Based Assessment of Breast Cancer–Related Lymphoedema Tissue Composition. Investigative Radiology, 2017, 52, 554-561.	3.5	30
43	T2-Weighted 4D Magnetic Resonance Imaging for Application in Magnetic Resonance–Guided Radiotherapy Treatment Planning. Investigative Radiology, 2017, 52, 563-573.	3.5	29
44	Feasibility and applicability of diffusion-weighted and dynamic contrast-enhanced magnetic resonance imaging in routine assessments of children with high-grade gliomas. Pediatric Blood and Cancer, 2017, 64, 279-283.	0.8	2
45	Imaging biomarker roadmap for cancer studies. Nature Reviews Clinical Oncology, 2017, 14, 169-186.	12.5	792
46	Diffusion-weighted Imaging as a Treatment Response Biomarker for Evaluating Bone Metastases in Prostate Cancer: A Pilot Study. Radiology, 2017, 283, 168-177.	3.6	81
47	Blood transfusion during radical chemo-radiotherapy does not reduce tumour hypoxia in squamous cell cancer of the head and neck. British Journal of Cancer, 2017, 116, 28-35.	2.9	20
48	Magnetic Resonance Spectroscopy to Study Glycolytic Metabolism During Autophagy. Methods in Enzymology, 2017, 588, 133-153.	0.4	10
49	Non-Invasive Prostate Cancer Characterization with Diffusion-Weighted MRI: Insight from In silico Studies of a Transgenic Mouse Model. Frontiers in Oncology, 2017, 7, 290.	1.3	7
50	Pediatric and adult glioblastoma radiosensitization induced by PI3K/mTOR inhibition causes early metabolic alterations detected by nuclear magnetic resonance spectroscopy. Oncotarget, 2017, 8, 47969-47983.	0.8	11
51	In vitro nuclear magnetic resonance spectroscopy metabolic biomarkers for the combination of temozolomide with PI3K inhibition in paediatric glioblastoma cells. PLoS ONE, 2017, 12, e0180263.	1.1	4
52	Evaluation of the combination of the dual m-TORC1/2 inhibitor vistusertib (AZD2014) and paclitaxel in ovarian cancer models. Oncotarget, 2017, 8, 113874-113884.	0.8	22
53	MRI Applications, Clinical. , 2017, , 873-882.		0
54	Abstract 444: Monocarboxylate transporter 1 inhibition with AZD3965 increases cancer cell dependence on bioenergetic metabolism predicating combination therapy with mitochondrial inhibitors. , 2017, , .		0

#	Article	IF	CITATIONS
55	Comparison of Dixon Sequences for Estimation of Percent Breast Fibroglandular Tissue. PLoS ONE, 2016, 11, e0152152.	1.1	17
56	Inter- and Intra-Observer Repeatability of Quantitative Whole-Body, Diffusion-Weighted Imaging (WBDWI) in Metastatic Bone Disease. PLoS ONE, 2016, 11, e0153840.	1.1	40
57	RA-02DIFFUSION-WEIGHTED AND DYNAMIC CONTRAST-ENHANCED MAGNETIC RESONANCE IMAGING AS MARKERS OF CLINICAL BEHAVIOUR IN PAEDIATRIC HIGH GRADE GLIOMAS. Neuro-Oncology, 2016, 18, iii165.1-iii165.	0.6	0
58	Evaluating the diagnostic sensitivity of computed diffusionâ€weighted MR imaging in the detection of breast cancer. Journal of Magnetic Resonance Imaging, 2016, 44, 130-137.	1.9	35
59	Quality assurance in MRI breast screening: comparing signal-to-noise ratio in dynamic contrast-enhanced imaging protocols. Physics in Medicine and Biology, 2016, 61, 37-49.	1.6	6
60	Modulation of renal oxygenation and perfusion in rat kidney monitored by quantitative diffusion and blood oxygen level dependent magnetic resonance imaging on a clinical 1.5T platform. BMC Nephrology, 2016, 17, 142.	0.8	6
61	Development of a temperatureâ€controlled phantom for magnetic resonance quality assurance of diffusion, dynamic, and relaxometry measurements. Medical Physics, 2016, 43, 2998-3007.	1.6	26
62	Extended T2-IVIM model for correction of TE dependence of pseudo-diffusion volume fraction in clinical diffusion-weighted magnetic resonance imaging. Physics in Medicine and Biology, 2016, 61, N667-N680.	1.6	54
63	A novel approach to evaluate spatial resolution of MRI clinical images for optimization and standardization of breast screening protocols. Medical Physics, 2016, 43, 6354-6363.	1.6	5
64	Visualizing whole-body treatment response heterogeneity using multi-parametric magnetic resonance imaging. Journal of Algorithms and Computational Technology, 2016, 10, 290-301.	0.4	15
65	Lactate and choline metabolites are potential biomarkers for monitoring response to mTOR pathway inhibitors in combination with the ALK inhibitor crizotinib in ALK-mutated neuroblastoma. European Journal of Cancer, 2016, 69, S25.	1.3	0
66	Volume of Bone Metastasis Assessed with Whole-Body Diffusion-weighted Imaging Is Associated with Overall Survival in Metastatic Castration-resistant Prostate Cancer. Radiology, 2016, 280, 151-160.	3.6	51
67	Pseudoprogression in children, adolescents and young adults with non-brainstem high grade glioma and diffuse intrinsic pontine glioma. Journal of Neuro-Oncology, 2016, 129, 109-121.	1.4	30
68	Repeatability and sensitivity of measurements in patients with head and neck squamous cell carcinoma at 3T. Journal of Magnetic Resonance Imaging, 2016, 44, 72-80.	1.9	27
69	Slice Encoding for Metal Artefact Correction in magnetic resonance imaging examinations for radiotherapy planning. Radiotherapy and Oncology, 2016, 120, 356-362.	0.3	10
70	T 2 -adjusted computed diffusion-weighted imaging: A novel method to enhance tumour visualisation. Computers in Biology and Medicine, 2016, 79, 92-98.	3.9	9
71	Validating a robust doubleâ€quantumâ€filtered <sup>1</sup> H MRS lactate measurement method in highâ€grade brain tumours. NMR in Biomedicine, 2016, 29, 1420-1426.	1.6	10
72	The BRAF Inhibitor Vemurafenib Activates Mitochondrial Metabolism and Inhibits Hyperpolarized Pyruvate–Lactate Exchange in BRAF-Mutant Human Melanoma Cells. Molecular Cancer Therapeutics, 2016, 15, 2987-2999.	1.9	43

#	Article	IF	CITATIONS
73	BRAF inhibition promotes BRAF mutant human melanoma cell survival under nutrient-deprived conditions through activation of mitochondrial metabolism. European Journal of Cancer, 2016, 61, S104.	1.3	0
74	Timeâ€resolved angiography with stochastic trajectories for dynamic contrastâ€enhanced MRI in head and neck cancer: Are pharmacokinetic parameters affected?. Medical Physics, 2016, 43, 6024-6032.	1.6	3
75	Pre-natal exposures and breast tissue composition: findings from a British pre-birth cohort of young women and a systematic review. Breast Cancer Research, 2016, 18, 102.	2.2	14
76	Assessment of repeatability and treatment response in early phase clinical trials using DCE-MRI: comparison of parametric analysis using MR- and CT-derived arterial input functions. European Radiology, 2016, 26, 1991-1998.	2.3	34
77	Rapid development of image analysis research tools: Bridging the gap between researcher and clinician with pyOsiriX. Computers in Biology and Medicine, 2016, 69, 203-212.	3.9	34
78	Contribution of mammography to MRI screening in BRCA mutation carriers by BRCA status and age: individual patient data meta-analysis. British Journal of Cancer, 2016, 114, 631-637.	2.9	99
79	Diffusion-weighted MR imaging of metastatic abdominal and pelvic tumours is sensitive to early changes induced by a VEGF inhibitor using alternative diffusion attenuation models. European Radiology, 2016, 26, 1412-1419.	2.3	36
80	Abstract B56: Treatment-induced autophagy increases amino acid uptake and switches glucose addiction to amino acid catabolism in cancer. , 2016, , .		1
81	Abstract B10: Noninvasive pharmacodynamic markers of the dual mTORC1/2 inhibitor AZD2014 in combination with paclitaxel, in cisplatin-resistant ovarian carcinoma xenografts. , 2016, , .		0
82	Abstract 3973: Diffusion-weighted imaging of bone metastases as treatment response biomarker in prostate cancer. , 2016, , .		0
83	Evaluation of lactate detection using selective multiple quantum coherence in phantoms and brain tumours. NMR in Biomedicine, 2015, 28, 338-343.	1.6	8
84	Singleâ€shot singleâ€voxel lactate measurements using FOClâ€LASER and a multipleâ€quantum filter. NMR in Biomedicine, 2015, 28, 496-504.	1.6	12
85	Multiâ€eentre reproducibility of diffusion MRI parameters for clinical sequences in the brain. NMR in Biomedicine, 2015, 28, 468-485.	1.6	178
86	Evaluation of diffusion models in breast cancer. Medical Physics, 2015, 42, 4833-4839.	1.6	16
87	Prospective, longitudinal, multi-modal functional imaging for radical chemo-IMRT treatment of locally advanced head and neck cancer: the INSIGHT study. Radiation Oncology, 2015, 10, 112.	1.2	15
88	High resolution 3D dosimetry for microbeam radiation therapy using optical CT. Journal of Physics: Conference Series, 2015, 573, 012032.	0.3	1
89	PRESAGE <sup>®</sup> as a new calibration method for high intensity focused ultrasound therapy. Journal of Physics: Conference Series, 2015, 573, 012026.	0.3	2
90	Use of the temporal median and trimmed mean mitigates effects of respiratory motion in multiple-acquisition abdominal diffusion imaging. Physics in Medicine and Biology, 2015, 60, N9-N20.	1.6	7

#	Article	IF	CITATIONS
91	Acting on incidental findings in research imaging. BMJ, The, 2015, 351, h5190-h5190.	3.0	36
92	Magnetic Resonance Imaging Improves Breast Screening Sensitivity in <i>BRCA</i> Mutation Carriers Age ≥ 50 Years: Evidence From an Individual Patient Data Meta-Analysis. Journal of Clinical Oncology, 2015, 33, 349-356.	0.8	72
93	First MRI application of an active breathing coordinator. Physics in Medicine and Biology, 2015, 60, 1681-1696.	1.6	12
94	Detecting microvascular changes in the mouse spleen using optical computed tomography. Microvascular Research, 2015, 101, 96-102.	1.1	2
95	Demonstration of the reproducibility of free-breathing diffusion-weighted MRI and dynamic contrast enhanced MRI in children with solid tumours: a pilot study. European Radiology, 2015, 25, 2641-2650.	2.3	22
96	Diffusion-weighted MR neurography for the assessment of brachial plexopathy in oncological practice. Cancer Imaging, 2015, 15, 6.	1.2	23
97	Quantitative Contrast-Enhanced Magnetic Resonance Lymphangiography of the Upper Limbs in Breast Cancer Related Lymphedema: An Exploratory Study. Lymphatic Research and Biology, 2015, 13, 100-106.	0.5	25
98	Acquired resistance to EGFR tyrosine kinase inhibitors alters the metabolism of human head and neck squamous carcinoma cells and xenograft tumours. British Journal of Cancer, 2015, 112, 1206-1214.	2.9	21
99	Response evaluation in mesothelioma: Beyond RECIST. Lung Cancer, 2015, 90, 433-441.	0.9	25
100	Phase I Study of Nintedanib Incorporating Dynamic Contrast-Enhanced Magnetic Resonance Imaging in Patients With Advanced Solid Tumors. Oncologist, 2015, 20, 368-369.	1.9	5
101	Characterizing Heterogeneity within Head and Neck Lesions Using Cluster Analysis of Multi-Parametric MRI Data. PLoS ONE, 2015, 10, e0138545.	1.1	6
102	Abstract CT138: Translating preclinical observations to the clinic: Combination of the dual m-TORC1/2 inhibitor AZD2014 and paclitaxel in ovarian and lung cancer. , 2015, , .		1
103	Abstract 1158: Real-time assessment of uptake and utilization of lactate in intact human breast cancer cells using a 1H-NMR-based assay. , 2015, , .		Ο
104	Abstract 1130: Unveiling the metabolic response of BRAF mutant melanoma cells to BRAF inhibition. , 2015, , .		0
105	Abstract 2897: Phosphatidylcholine synthesis is required for autophagosome membrane formation and maintenance during autophagy. , 2015, , .		0
106	Abstract C113: The monocarboxylate transporter 1 (MCT1) inhibitor AZD3965 triggers MCT4-dependent lactate accumulation and blocks pyruvate-lactate exchange in human cancer cells. , 2015, , .		0
107	Assessment of Treatment Response by Total Tumor Volume and Global Apparent Diffusion Coefficient Using Diffusion-Weighted MRI in Patients with Metastatic Bone Disease: A Feasibility Study. PLoS ONE, 2014, 9, e91779.	1.1	104
108	Reduced Warburg Effect in Cancer Cells Undergoing Autophagy: Steady- State 1H-MRS and Real-Time Hyperpolarized 13C-MRS Studies. PLoS ONE, 2014, 9, e92645.	1.1	17

#	Article	IF	CITATIONS
109	Investigating the Influence of Flip Angle and k-Space Sampling on Dynamic Contrast-Enhanced MRI Breast Examinations. Academic Radiology, 2014, 21, 1394-1401.	1.3	8
110	Dichloroacetate induces autophagy in colorectal cancer cells and tumours. British Journal of Cancer, 2014, 111, 375-385.	2.9	79
111	Interrogating Two Schedules of the AKT Inhibitor MK-2206 in Patients with Advanced Solid Tumors Incorporating Novel Pharmacodynamic and Functional Imaging Biomarkers. Clinical Cancer Research, 2014, 20, 5672-5685.	3.2	66
112	Development of a Hybrid Magnetic Resonance and Ultrasound Imaging System. BioMed Research International, 2014, 2014, 1-16.	0.9	6
113	Comparison of freeâ€breathing with navigatorâ€controlled acquisition regimes in abdominal diffusionâ€weighted magnetic resonance images: Effect on ADC and IVIM statistics. Journal of Magnetic Resonance Imaging, 2014, 39, 235-240.	1.9	61
114	MRI breast screening in high-risk women: cancer detection and survival analysis. Breast Cancer Research and Treatment, 2014, 145, 663-672.	1.1	133
115	Quantitative PET and SPECT performance characteristics of the Albira Trimodal pre-clinical tomograph. Physics in Medicine and Biology, 2014, 59, 715-731.	1.6	25
116	Comparison of three reference methods for the measurement of intracellular pH using <sup>31</sup> P MRS in healthy volunteers and patients with lymphoma. NMR in Biomedicine, 2014, 27, 158-162.	1.6	26
117	Clinical Proton MR Spectroscopy in Central Nervous System Disorders. Radiology, 2014, 270, 658-679.	3.6	524
118	Improved intravoxel incoherent motion analysis of diffusion weighted imaging by data driven Bayesian modeling. Magnetic Resonance in Medicine, 2014, 71, 411-420.	1.9	107
119	Lactate and Choline Metabolites Detected In Vitro by Nuclear Magnetic Resonance Spectroscopy Are Potential Metabolic Biomarkers for PI3K Inhibition in Pediatric Glioblastoma. PLoS ONE, 2014, 9, e103835.	1.1	21
120	Abstract 2451: Insulin-like growth factor-1 receptor (IGF-1R) inhibitors downregulate p53 expression and upregulate the Warburg effect in paediatric glioblastoma cells. , 2014, , .		0
121	Breast dynamic contrast-enhanced examinations with fat suppression: Are contrast-agent uptake curves affected by magnetic field inhomogeneity?. European Radiology, 2013, 23, 1537-1545.	2.3	6
122	Critical research gaps and translational priorities for the successful prevention and treatment of breast cancer. Breast Cancer Research, 2013, 15, R92.	2.2	320
123	Acute tumour response to the MEK1/2 inhibitor selumetinib (AZD6244, ARRY-142886) evaluated by non-invasive diffusion-weighted MRI. British Journal of Cancer, 2013, 109, 1562-1569.	2.9	22
124	Stacked Autoencoders for Unsupervised Feature Learning and Multiple Organ Detection in a Pilot Study Using 4D Patient Data. IEEE Transactions on Pattern Analysis and Machine Intelligence, 2013, 35, 1930-1943.	9.7	458
125	Measurement reproducibility of perfusion fraction and pseudodiffusion coefficient derived by intravoxel incoherent motion diffusion-weighted MR imaging in normal liver and metastases. European Radiology, 2013, 23, 428-434.	2.3	251
126	Noninvasive Phosphorus Magnetic Resonance Spectroscopic Imaging Predicts Outcome to First-line Chemotherapy in Newly Diagnosed Patients with Diffuse Large B-Cell Lymphoma. Academic Radiology, 2013, 20, 1122-1129.	1.3	9

#	Article	IF	CITATIONS
127	Multi-Frame SPRITE: A method for resolution enhancement of multiple-point SPRITE data. Journal of Magnetic Resonance, 2013, 230, 111-116.	1.2	12
128	Reproducibility of Dynamic Contrast-enhanced MR Imaging: Why We Should Care. Radiology, 2013, 266, 698-700.	3.6	18
129	The role of pre-treatment diffusion-weighted MRI in predicting long-term outcome of colorectal liver metastasis. British Journal of Radiology, 2013, 86, 20130281.	1.0	32
130	First-in-Human Phase I Trial of Two Schedules of OSI-930, a Novel Multikinase Inhibitor, Incorporating Translational Proof-of-Mechanism Studies. Clinical Cancer Research, 2013, 19, 909-919.	3.2	26
131	1 H NMR and hyperpolarized 13 C NMR assays of pyruvate–lactate: a comparative study. NMR in Biomedicine, 2013, 26, 1321-1325.	1.6	25
132	Optimal age to start preventive measures in women with <i>BRCA1/2</i> mutations or high familial breast cancer risk. International Journal of Cancer, 2013, 133, 156-163.	2.3	20
133	MEK1/2 Inhibition Decreases Lactate in BRAF-Driven Human Cancer Cells. Cancer Research, 2013, 73, 4039-4049.	0.4	40
134	Profiling metabolite changes in the neuronal differentiation of human striatal neural stem cells using 1H-magnetic resonance spectroscopy. NeuroReport, 2013, 24, 1035-1040.	0.6	8
135	Wireless Accelerometer for MRI-Guided Interventional Procedures. Technologies, 2013, 1, 44-53.	3.0	2
136	Model Free Approach to Kinetic Analysis of Real-Time Hyperpolarized 13C Magnetic Resonance Spectroscopy Data. PLoS ONE, 2013, 8, e71996.	1.1	134
137	Abstract 5640: Picropodophyllin downregulates p53 and increases the Warburg effect in pediatric glioblastoma cells , 2013, , .		0
138	Phase I Trial of Combretastatin A4 Phosphate (CA4P) in Combination with Bevacizumab in Patients with Advanced Cancer. Clinical Cancer Research, 2012, 18, 3428-3439.	3.2	158
139	Appearances of colorectal hepatic metastases at diffusion-weighted MRI compared with histopathology: initial observations. British Journal of Radiology, 2012, 85, 225-230.	1.0	18
140	Histone Deacetylase Inhibition Increases Levels of Choline Kinase α and Phosphocholine Facilitating Noninvasive Imaging in Human Cancers. Cancer Research, 2012, 72, 990-1000.	0.4	23
141	Common Breast Cancer Susceptibility Variants in <i>LSP1</i> and <i>RAD51L1</i> Are Associated with Mammographic Density Measures that Predict Breast Cancer Risk. Cancer Epidemiology Biomarkers and Prevention, 2012, 21, 1156-1166.	1.1	101
142	Informatics in Radiology: Development of a Research PACS for Analysis of Functional Imaging Data in Clinical Research and Clinical Trials. Radiographics, 2012, 32, 2135-2150.	1.4	18
143	Neuroendocrine Tumor Liver Metastases: Use of Dynamic Contrast-enhanced MR Imaging to Monitor and Predict Radiolabeled Octreotide Therapy Response. Radiology, 2012, 263, 139-148.	3.6	40
144	Advanced Solid Tumors Treated with Cediranib: Comparison of Dynamic Contrast-enhanced MR Imaging and CT as Markers of Vascular Activity. Radiology, 2012, 265, 426-436.	3.6	51

#	Article	IF	CITATIONS
145	Differences in Natural History between Breast Cancers in <i>BRCA1</i> and <i>BRCA2</i> Mutation Carriers and Effects of MRI Screening-MRISC, MARIBS, and Canadian Studies Combined. Cancer Epidemiology Biomarkers and Prevention, 2012, 21, 1458-1468.	1.1	79
146	Combination of chemical suppression techniques for dual suppression of fat and silicone at diffusion-weighted MR imaging in women with breast implants. European Radiology, 2012, 22, 2648-2653.	2.3	14
147	Evaluation of distortion correction of diffusion-weighted MR images of human cervix. , 2012, , .		2
148	Assessment of colorectal hepatic metastases by quantitative T2 relaxation time. European Journal of Radiology, 2012, 81, e536-e540.	1.2	8
149	Effects of HSP90 inhibitor 17-allylamino-17-demethoxygeldanamycin (17-AAG) on NEU/HER2 overexpressing mammary tumours in MMTV-NEU-NT mice monitored by Magnetic Resonance Spectroscopy. BMC Research Notes, 2012, 5, 250.	0.6	13
150	Functional imaging in adult and paediatric brain tumours. Nature Reviews Clinical Oncology, 2012, 9, 700-711.	12.5	58
151	Whole-Body Diffusion-Weighted MRI: Tips, Tricks, and Pitfalls. American Journal of Roentgenology, 2012, 199, 252-262.	1.0	158
152	Imaging vascular function for early stage clinical trials using dynamic contrast-enhanced magnetic resonance imaging. European Radiology, 2012, 22, 1451-1464.	2.3	138
153	An evaluation of motion compensation strategies and repeatability for abdominal <sup>1</sup> H MR spectroscopy measurements in volunteer studies and clinical trials. NMR in Biomedicine, 2012, 25, 859-865.	1.6	9
154	Abstract B61: Picropodophyllin (PPP) increases glucose metabolism and lactate production in paediatric glioblastoma cells. Clinical Cancer Research, 2012, 18, B61-B61.	3.2	1
155	Abstract 2501: Inhibition of the PI3K pathway potentiates temozolomide effects in pediatric glioblastoma and results in alterations in glucose and choline metabolism detected by MRS. , 2012, , .		0
156	Analysis of Cancer Metabolism by Imaging Hyperpolarized Nuclei: Prospects for Translation to Clinical Research. Neoplasia, 2011, 13, 81-97.	2.3	623
157	Psychological impact and acceptability of magnetic resonance imaging and X-ray mammography: the MARIBS Study. British Journal of Cancer, 2011, 104, 578-586.	2.9	22
158	A Bayesian hierarchical model for DCE-MRI to evaluate treatment response in a phase II study in advanced squamous cell carcinoma of the head and neck. Magnetic Resonance Materials in Physics, Biology, and Medicine, 2011, 24, 85-96.	1.1	8
159	Dynamic contrastâ€enhanced MRI of neuroendocrine hepatic metastases: A feasibility study using a dualâ€input twoâ€compartment model. Magnetic Resonance in Medicine, 2011, 65, 250-260.	1.9	40
160	Noninvasive detection of carboxypeptidase G2 activity <i>in vivo</i> . NMR in Biomedicine, 2011, 24, 343-350.	1.6	11
161	Assessment of the effect of haematocritâ€dependent arterial input functions on the accuracy of pharmacokinetic parameters in dynamic contrastâ€enhanced MRI. NMR in Biomedicine, 2011, 24, 902-915.	1.6	19
162	Computed Diffusion-weighted MR Imaging May Improve Tumor Detection. Radiology, 2011, 261, 573-581.	3.6	148

#	Article	IF	CITATIONS
163	Autoencoder in Time-Series Analysis for Unsupervised Tissues Characterisation in a Large Unlabelled Medical Image Dataset. , 2011, , .		19
164	Phase I Trial of a Selective c-MET Inhibitor ARQ 197 Incorporating Proof of Mechanism Pharmacodynamic Studies. Journal of Clinical Oncology, 2011, 29, 1271-1279.	0.8	189
165	Exploiting tumor metabolism for non-invasive imaging of the therapeutic activity of molecularly targeted anticancer agents. Cell Cycle, 2011, 10, 2883-2893.	1.3	21
166	Computerized detection of breast lesions in multi-centre and multi-instrument DCE-MR data using 3D principal component maps and template matching. Physics in Medicine and Biology, 2011, 56, 7795-7811.	1.6	10
167	Quantitative diffusion-weighted (DW) MR imaging of microcapillary perfusion and tissue diffusivity as biomarkers of response of renal cell carcinoma (RCC) to treatment with sunitinib Journal of Clinical Oncology, 2011, 29, TPS154-TPS154.	0.8	4
168	Optimising magnetic resonance imaging for preoperative staging and surgical planning in colon cancer at 1.5 tesla and 3.0 tesla Journal of Clinical Oncology, 2011, 29, 395-395.	0.8	0
169	Abstract 3788: Autophagy induced by DCA, PI3K inhibition or starvation results in reduced lactate production measured in real-time by DNP 13C MRS. , 2011, , .		0
170	Abstract 5277: Non-invasive metabolic biomarkers of histone deacetylase inhibition in human colon cancer cells and tumors. , 2011, , .		0
171	Metabolic assessment of the action of targeted cancer therapeutics using magnetic resonance spectroscopy. British Journal of Cancer, 2010, 102, 1-7.	2.9	67
172	Virtual conferences becoming a reality. Nature Chemistry, 2010, 2, 148-152.	6.6	28
173	The Phosphoinositide 3-Kinase Inhibitor Pl-103 Downregulates Choline Kinase α Leading to Phosphocholine and Total Choline Decrease Detected by Magnetic Resonance Spectroscopy. Cancer Research, 2010, 70, 5507-5517.	0.4	58
174	Modulation of melanoma cell phospholipid metabolism in response to heat shock protein 90 inhibition. Oncotarget, 2010, 1, 185-197.	0.8	22
175	Robustness of interactive intensity thresholding based breast density assessment in MR-mammography. Proceedings of SPIE, 2010, , .	0.8	0
176	Abstract 5083: Inhibition of MEK1/2 signaling in humanBRAFV600Emelanoma cells reduces glucose uptake and lactate dehydrogenase activity resulting in a time-dependent decrease in lactate production. , 2010, , .		0
177	Correlation of the intra-tumor phospholipid-related signatures determined noninvasively by phosphorus and hydrogen MR spectroscopy: An approach to increase the sensitivity and applicability of the technique to predict therapeutic outcome in non-Hodgkin's lymphoma Journal of Clinical Oncology, 2010, 28, 8070-8070.	0.8	0
178	Phosphorus Magnetic Resonance Spectroscopy Predicts Outcome to Chemotherapy In Patients with Diffuse Large B-Cell Lymphoma: A Prospective International Multicenter Analysis of a Pretreatment Metabolic Biomarker of Response. Blood, 2010, 116, 3104-3104.	0.6	0
179	Changes in choline metabolism as potential biomarkers of phospholipase CÎ <sup>3</sup> 1 inhibition in human prostate cancer cells. Molecular Cancer Therapeutics, 2009, 8, 1305-1311.	1.9	24
180	Optimizing functional parameter accuracy for breath-hold DCE-MRI of liver tumours. Physics in Medicine and Biology, 2009, 54, 2197-2215.	1.6	28

#	Article	IF	CITATIONS
181	Eligibility for Magnetic Resonance Imaging Screening in the United Kingdom: Effect of Strict Selection Criteria and Anonymous DNA Testing on Breast Cancer Incidence in the MARIBS Study. Cancer Epidemiology Biomarkers and Prevention, 2009, 18, 2123-2131.	1.1	14
182	Dynamic contrast-enhanced MRI for prostate cancer localization. British Journal of Radiology, 2009, 82, 148-156.	1.0	93
183	Cancers in <i>BRCA1</i> and <i>BRCA2</i> Carriers and in Women at High Risk for Breast Cancer: MR Imaging and Mammographic Features. Radiology, 2009, 252, 358-368.	3.6	67
184	Modulating the relaxivity of hyperpolarized substrates with gadolinium contrast agents. Contrast Media and Molecular Imaging, 2009, 4, 143-147.	0.4	19
185	Motion artifact correction in freeâ€breathing abdominal MRI using overlapping partial samples to recover image deformations. Magnetic Resonance in Medicine, 2009, 62, 440-449.	1.9	22
186	Hyperpolarized <sup>13</sup> C magnetic resonance detection of carboxypeptidase G2 activity. Magnetic Resonance in Medicine, 2009, 62, 1300-1304.	1.9	36
187	Breast cancer screening in women at high risk using MRI. NMR in Biomedicine, 2009, 22, 17-27.	1.6	26
188	Modulation of choline kinase activity in human cancer cells observed by dynamic <sup>31</sup> P NMR. NMR in Biomedicine, 2009, 22, 456-461.	1.6	16
189	A novel technique to monitor carboxypeptidase G2 expression in suicide gene therapy using <sup>19</sup> F magnetic resonance spectroscopy. NMR in Biomedicine, 2009, 22, 561-566.	1.6	9
190	An Exploratory Study Into the Role of Dynamic Contrast-Enhanced Magnetic Resonance Imaging or Perfusion Computed Tomography for Detection of Intratumoral Hypoxia in Head-and-Neck Cancer. International Journal of Radiation Oncology Biology Physics, 2009, 74, 29-37.	0.4	82
191	A phase I study of the nitroimidazole hypoxia marker SR4554 using 19F magnetic resonance spectroscopy. British Journal of Cancer, 2009, 101, 1860-1868.	2.9	34
192	Phase-cycled averaging for the suppression of residual magnetisation in SPI sequences. Journal of Magnetic Resonance, 2009, 199, 117-125.	1.2	6
193	Reproducibility and changes in the apparent diffusion coefficients of solid tumours treated with combretastatin A4 phosphate and bevacizumab in a two-centre phase I clinical trial. European Radiology, 2009, 19, 2728-2738.	2.3	151
194	Quantitative imaging biomarkers in neuro-oncology. Nature Reviews Clinical Oncology, 2009, 6, 445-454.	12.5	92
195	Assessing the usefulness of a novel MRI-based breast density estimation algorithm in a cohort of women at high genetic risk of breast cancer: the UK MARIBS study. Breast Cancer Research, 2009, 11, R80.	2.2	77
196	Comparison of Breast Density Assessments Based on Interactive Thresholding and Automated Fast Fuzzy c-means Clustering in Three-Dimensional MR Imaging. IFMBE Proceedings, 2009, , 1893-1896.	0.2	3
197	Prediction of treatment response in subtypes of non-Hodgkin's lymphoma by in vivo <sup>31</sup> P MR spectroscopy before treatment. Journal of Clinical Oncology, 2009, 27, 8565-8565.	0.8	1
198	Abstract A72: Assessment of pyuvate dehydrogenase kinase inhibition by dichloroacetate in human colon carcinoma cells by dynamic hyperpolarized13C MRS and steady state1H MRS. , 2009, , .		0

#	Article	IF	CITATIONS
199	Abstract A224: Noninvasive PD markers of a pyruvate dehydrogenase kinase inhibitor, dichloroacetate, in human colon carcinoma xenografts. , 2009, , .		0
200	Abstract A228: Noninvasive magnetic resonance spectroscopic PD markers of a minorâ€groove interstrand crossâ€linking agent (BN2629) in human colon carcinoma and melanoma xenografts. , 2009, , ·		0
201	Detection of colorectal hepatic metastases using MnDPDP MR imaging and diffusion-weighted imaging (DWI) alone and in combination. European Radiology, 2008, 18, 903-910.	2.3	145
202	Quantitative mapping of hepatic perfusion index using MR imaging: a potential reproducible tool for assessing tumour response to treatment with the antiangiogenic compound BIBF 1120, a potent triple angiokinase inhibitor. European Radiology, 2008, 18, 1414-1421.	2.3	39
203	80 POSTER Inhibition of MEK1/2 signalling results in decreased levels of intracellular lactate in human melanoma and colorectal cancer cells as observed with magnetic resonance spectroscopy. European Journal of Cancer, Supplement, 2008, 6, 27-28.	2.2	0
204	Noninvasive Magnetic Resonance Spectroscopic Pharmacodynamic Markers of a Novel Histone Deacetylase Inhibitor, LAQ824, in Human Colon Carcinoma Cells and Xenografts. Neoplasia, 2008, 10, 303-313.	2.3	41
205	Computationally efficient vascular input function models for quantitative kinetic modelling using DCE-MRI. Physics in Medicine and Biology, 2008, 53, 1225-1239.	1.6	114
206	Therapeutic Target Metabolism Observed Using Hyperpolarized <sup>15</sup> N Choline. Journal of the American Chemical Society, 2008, 130, 4598-4599.	6.6	116
207	A Pilot Study of Compositional Analysis of the Breast and Estimation of Breast Mammographic Density Using Three-Dimensional T1-Weighted Magnetic Resonance Imaging. Cancer Epidemiology Biomarkers and Prevention, 2008, 17, 2268-2274.	1.1	81
208	The value of magnetic resonance spectroscopy in tumour imaging. Archives of Disease in Childhood, 2008, 93, 725-727.	1.0	21
209	Bayesian estimation of pharmacokinetic parameters for DCE-MRI with a robust treatment of enhancement onset time. Physics in Medicine and Biology, 2007, 52, 2393-2408.	1.6	34
210	Reference tissue quantification of DCE-MRI data without a contrast agent calibration. Physics in Medicine and Biology, 2007, 52, 589-601.	1.6	36
211	BRCA1 Mutation and Young Age Predict Fast Breast Cancer Growth in the Dutch, United Kingdom, and Canadian Magnetic Resonance Imaging Screening Trials. Clinical Cancer Research, 2007, 13, 7357-7362.	3.2	97
212	Distortion-corrected <i>T</i> <sub>2</sub> weighted MRI: a novel approach to prostate radiotherapy planning. British Journal of Radiology, 2007, 80, 926-933.	1.0	20
213	EU Directive 2004/40: field measurements of a 1.5â€T clinical MR scanner. British Journal of Radiology, 2007, 80, 483-487.	1.0	22
214	Parametric mapping of the hepatic perfusion index with gadolinium-enhanced volumetric MRI. British Journal of Radiology, 2007, 80, 113-120.	1.0	19
215	Predicting Response of Colorectal Hepatic Metastasis: Value of Pretreatment Apparent Diffusion Coefficients. American Journal of Roentgenology, 2007, 188, 1001-1008.	1.0	324
216	Registration of dynamic contrast-enhanced MRI using a progressive principal component registration (PPCR). Physics in Medicine and Biology, 2007, 52, 5147-5156.	1.6	89

#	Article	IF	CITATIONS
217	Quantitative evaluation of free-form deformation registration for dynamic contrast-enhanced MR mammography. Medical Physics, 2007, 34, 1221-1233.	1.6	36
218	Reproducibility of reference tissue quantification of dynamic contrast-enhanced data: comparison with a fixed vascular input function. Physics in Medicine and Biology, 2007, 52, 75-89.	1.6	52
219	Selective homonuclear Hartmann–Hahn for <sup>13</sup> C→ <sup>13</sup> C polarization transfer in solution state NMR. Molecular Physics, 2007, 105, 1827-1832.	0.8	1
220	Conformational exchange in pimonidazole—a hypoxia marker. Magnetic Resonance in Chemistry, 2007, 45, 621-623.	1.1	3
221	Dynamic MRI for imaging tumor microvasculature: Comparison of susceptibility and relaxivity techniques in pelvic tumors. Journal of Magnetic Resonance Imaging, 2007, 25, 796-805.	1.9	48
222	Measurements of occupational exposure to switched gradient and spatially-varying magnetic fields in areas adjacent to 1.5T clinical MRI systems. Journal of Magnetic Resonance Imaging, 2007, 26, 1346-1352.	1.9	32
223	Multiscale analysis of MR-mammography data. Zeitschrift Fur Medizinische Physik, 2007, 17, 166-171.	0.6	0
224	American Cancer Society Guidelines for Breast Screening with MRI as an Adjunct to Mammography. Ca-A Cancer Journal for Clinicians, 2007, 57, 75-89.	157.7	2,234
225	Applications of magnetic resonance spectroscopy in radiotherapy treatment planning. British Journal of Radiology, 2006, 79, S16-S26.	1.0	87
226	Evaluation of response to treatment using DCE-MRI: the relationship between initial area under the gadolinium curve (IAUGC) and quantitative pharmacokinetic analysis. Physics in Medicine and Biology, 2006, 51, 3593-3602.	1.6	115
227	An investigation of dose calculation accuracy in intensity-modulated radiotherapy of sites in the head & neck. Physica Medica, 2006, 22, 97-104.	0.4	10
228	A test of performance of breast MRI interpretation in a multicentre screening study. Magnetic Resonance Imaging, 2006, 24, 917-929.	1.0	16
229	Application of the chirp z-transform to MRI data. Journal of Magnetic Resonance, 2006, 178, 121-128.	1.2	21
230	Colorectal hepatic metastases: quantitative measurements using single-shot echo-planar diffusion-weighted MR imaging. European Radiology, 2006, 16, 1898-1905.	2.3	123
231	Evaluation of 31P high-resolution magic angle spinning of intact tissue samples. NMR in Biomedicine, 2006, 19, 593-598.	1.6	29
232	In vivo31P MR spectral patterns and reproducibility in cancer patients studied in a multi-institutional trial. NMR in Biomedicine, 2006, 19, 504-512.	1.6	56
233	Magnetic Resonance Imaging Workbench: Analysis and Visualization of Dynamic Contrast-enhanced MR Imaging Data. Radiographics, 2006, 26, 621-632.	1.4	82
234	Evaluation of a Prospective Scoring System Designed for a Multicenter Breast MR Imaging Screening Study. Radiology, 2006, 239, 677-685.	3.6	29

#	Article	IF	CITATIONS
235	Magnetic resonance spectroscopy (MRS) in the investigation of cancer at The Royal Marsden Hospital and The Institute of Cancer Research. Physics in Medicine and Biology, 2006, 51, R61-R82.	1.6	13
236	Prediction of Clinicopathologic Response of Breast Cancer to Primary Chemotherapy at Contrast-enhanced MR Imaging: Initial Clinical Results. Radiology, 2006, 239, 361-374.	3.6	224
237	Identification of magnetic resonance detectable metabolic changes associated with inhibition of phosphoinositide 3-kinase signaling in human breast cancer cells. Molecular Cancer Therapeutics, 2006, 5, 187-196.	1.9	84
238	Minimally Invasive Pharmacokinetic and Pharmacodynamic Technologies in Hypothesis-Testing Clinical Trials of Innovative Therapies. Journal of the National Cancer Institute, 2006, 98, 580-598.	3.0	189
239	Noninvasive Magnetic Resonance Spectroscopic Pharmacodynamic Markers of the Choline Kinase Inhibitor MN58b in Human Carcinoma Models. Cancer Research, 2006, 66, 427-434.	0.4	135
240	Factors influencing the accuracy of biomechanical breast models. Medical Physics, 2006, 33, 1758-1769.	1.6	98
241	Cost-effectiveness of screening with contrast enhanced magnetic resonance imaging vs X-ray mammography of women at a high familial risk of breast cancer. British Journal of Cancer, 2006, 95, 801-810.	2.9	113
242	MRI for breast cancer screening. Annals of Oncology, 2006, 17, x325-x331.	0.6	7
243	Micro-coils for MR spectroscopy by deep silicon etching. Journal of Physics: Conference Series, 2005, 15, 13-18.	0.3	2
244	Adiabatic half-passage pulses for measuring the polarization of highly non-equilibrium spin-systems. Chemical Physics Letters, 2005, 414, 102-106.	1.2	1
245	Quantitative assessment of the hepatic pharmacokinetics of the antimicrobial sitafloxacin in humans using in vivo19F magnetic resonance spectroscopy. British Journal of Clinical Pharmacology, 2005, 59, 244-248.	1.1	15
246	The assessment of antiangiogenic and antivascular therapies in early-stage clinical trials using magnetic resonance imaging: issues and recommendations. British Journal of Cancer, 2005, 92, 1599-1610.	2.9	487
247	A Phase I study of the angiogenesis inhibitor SU5416 (semaxanib) in solid tumours, incorporating dynamic contrast MR pharmacodynamic end points. British Journal of Cancer, 2005, 93, 876-883.	2.9	75
248	Evaluation of radiological features for breast tumour classification in clinical screening with machine learning methods. Artificial Intelligence in Medicine, 2005, 34, 129-139.	3.8	53
249	Burst imaging—Can it ever be useful in the clinic?. Concepts in Magnetic Resonance Part A: Bridging Education and Research, 2005, 26A, 11-34.	0.2	7
250	Localized COSY and DQF-COSY1H-MRS sequences for investigating human tibial bone marrow in vivo and initial application to patients with acute leukemia. Journal of Magnetic Resonance Imaging, 2005, 22, 541-548.	1.9	25
251	Implementation and evaluation of CSI-localizedJ cross-polarization for detection of 31P magnetic resonance spectra in vivo. Magnetic Resonance in Medicine, 2005, 54, 1065-1071.	1.9	9
252	Antivascular cancer treatments: functional assessments by dynamic contrast-enhanced magnetic resonance imaging. Abdominal Imaging, 2005, 30, 325-342.	2.0	116

#	Article	IF	CITATIONS
253	Investigations in vivo of the effects of carbogen breathing on 5-fluorouracil pharmacokinetics and physiology of solid rodent tumours. Cancer Chemotherapy and Pharmacology, 2005, 55, 117-128.	1.1	11
254	Identification of biliary metabolites of ifosfamide using 31P magnetic resonance spectroscopy and mass spectrometry. Cancer Chemotherapy and Pharmacology, 2005, 56, 409-414.	1.1	8
255	Preliminary dose response study of a gel dosimeter using 2-Hydroxyethyl Methacrylate (HEMA). Australasian Physical and Engineering Sciences in Medicine, 2005, 28, 172-174.	1.4	10
256	Use of Dynamic Contrast-Enhanced MRI in Multi-Centre Trials with Particular Reference to Breast Cancer Screening in Women at Genetic Risk. , 2005, , 265-279.		0
257	Magnetic Resonance Spectroscopy Monitoring of Mitogen-Activated Protein Kinase Signaling Inhibition. Cancer Research, 2005, 65, 3356-3363.	0.4	80
258	Inversion recovery measurements in the presence of radiation damping and implications for evaluating contrast agents in magnetic resonance. Physics in Medicine and Biology, 2005, 50, N371-N376.	1.6	15
259	Dual-contrast echo planar imaging with keyhole: application to dynamic contrast-enhanced perfusion studies. Physics in Medicine and Biology, 2005, 50, 4491-4505.	1.6	19
260	A complete distortion correction for MR images: II. Rectification of static-field inhomogeneities by similarity-based profile mapping. Physics in Medicine and Biology, 2005, 50, 2651-2661.	1.6	86
261	A complete distortion correction for MR images: I. Gradient warp correction. Physics in Medicine and Biology, 2005, 50, 1343-1361.	1.6	201
262	Reading Protocol for Dynamic Contrast-enhanced MR Images of the Breast: Sensitivity and Specificity Analysis. Radiology, 2005, 236, 779-788.	3.6	99
263	Effects of platinum/taxane based chemotherapy on acute perfusion in human pelvic tumours measured by dynamic MRI. British Journal of Cancer, 2005, 93, 979-985.	2.9	30
264	Processing of radical prostatectomy specimens for correlation of data from histopathological, molecular biological, and radiological studies: a new whole organ technique. Journal of Clinical Pathology, 2005, 58, 504-508.	1.0	41
265	Screening with magnetic resonance imaging and mammography of a UK population at high familial risk of breast cancer: a prospective multicentre cohort study (MARIBS). Lancet, The, 2005, 365, 1769-1778.	6.3	927
266	Electromagnetic field exposure limitation and the future of MRI. British Journal of Radiology, 2005, 78, 973-973.	1.0	37
267	The use of gel dosimetry for verification of electron and photon treatment plans in carcinoma of the scalp. Physics in Medicine and Biology, 2004, 49, 1625-1635.	1.6	33
268	Measurement of the three-dimensional distribution of radiation dose in grid therapy. Physics in Medicine and Biology, 2004, 49, N317-N323.	1.6	17
269	Notices of Duplicate Publication. Radiology, 2004, 233, 938-938.	3.6	2
270	Noninvasive Measurements of Capecitabine Metabolism in Bladder Tumors Overexpressing Thymidine Phosphorylase by Fluorine-19 Magnetic Resonance Spectroscopy. Clinical Cancer Research, 2004, 10, 3863-3870.	3.2	19

#	Article	IF	CITATIONS
271	Investigation of microenvironmental factors influencing the longitudinal relaxation times of drugs and other compounds. Magnetic Resonance Imaging, 2004, 22, 973-982.	1.0	6
272	Methodological standardization for a multi-institutionalin vivo trial of localized31P MR spectroscopy in human cancer research.In vitro and normal volunteer studies. NMR in Biomedicine, 2004, 17, 382-391.	1.6	36
273	Effects of residual single-quantum coherences in intermolecular multiple-quantum coherence studies. Journal of Magnetic Resonance, 2004, 166, 215-227.	1.2	25
274	Dose resolution in gel dosimetry: effect of uncertainty in the calibration function. Physics in Medicine and Biology, 2004, 49, N139-N146.	1.6	28
275	Monitoring temozolomide treatment of low-grade glioma with proton magnetic resonance spectroscopy. British Journal of Cancer, 2004, 90, 781-786.	2.9	101
276	Developing a quality control protocol for diffusion imaging on a clinical MRI system. Physics in Medicine and Biology, 2004, 49, 1409-1422.	1.6	60
277	Image fusion for dynamic contrast enhanced magnetic resonance imaging. BioMedical Engineering OnLine, 2004, 3, 35.	1.3	27
278	Classification Improvement by Segmentation Refinement: Application to Contrast-Enhanced MR-Mammography. Lecture Notes in Computer Science, 2004, , 184-191.	1.0	4
279	Visualization of multivariate image data using image fusion and perceptually optimized color scales based on sRGB. , 2004, , .		0
280	Alignment of dynamic contrast-enhanced MR volumes of the breast for a multicenter trial: an exemplar grid application. , 2004, , .		0
281	Multiscale entropy analysis in dynamic contrast-enhanced MRI. , 2004, , .		0
282	Does vascular imaging with MRI predict response to neoadjuvant chemotherapy in primary breast cancer?. Journal of Clinical Oncology, 2004, 22, 582-582.	0.8	8
283	Does vascular imaging with MRI predict response to neoadjuvant chemotherapy in primary breast cancer?. Journal of Clinical Oncology, 2004, 22, 582-582.	0.8	0
284	Polymer gel measurement of dose homogeneity in the breast: comparing MLC intensity modulation with standard wedged delivery. Physics in Medicine and Biology, 2003, 48, 1065-1074.	1.6	19
285	Ifosfamide pharmacokinetics and hepatobiliary uptake in vivo investigated using single- and double-resonance31P MRS. Magnetic Resonance in Medicine, 2003, 50, 249-255.	1.9	7
286	Comparison of polarization transfer sequences for enhancement of signals in clinical31P MRS studies. Magnetic Resonance in Medicine, 2003, 50, 578-588.	1.9	18
287	Hyperpolarising 13C for NMR studies using laser-polarised 129Xe: SPINOE vs thermal mixing. Chemical Physics Letters, 2003, 371, 640-644.	1.2	23
288	Assessment of antiangiogenic and antivascular therapeutics using MRI: recommendations for appropriate methodology for clinical trials. British Journal of Radiology, 2003, 76, S87-S91.	1.0	121

#	Article	IF	CITATIONS
289	Radiotherapy treatment planning of prostate cancer using magnetic resonance imaging alone. Radiotherapy and Oncology, 2003, 66, 203-216.	0.3	300
290	Validation of nonrigid image registration using finite-element methods: application to breast MR images. IEEE Transactions on Medical Imaging, 2003, 22, 238-247.	5.4	224
291	Increased tumour extracellular pH induced by Bafilomycin A1 inhibits tumour growth and mitosis in vivo and alters 5-fluorouracil pharmacokinetics. European Journal of Cancer, 2003, 39, 532-540.	1.3	32
292	Potential role of magnetic resonance spectroscopy in assessment of tumour response in childhood cancer. European Journal of Cancer, 2003, 39, 728-735.	1.3	36
293	Magnetic Resonance Spectroscopic Pharmacodynamic Markers of the Heat Shock Protein 90 Inhibitor 17-Allylamino,17-Demethoxygeldanamycin (17AAG) in Human Colon Cancer Models. Journal of the National Cancer Institute, 2003, 95, 1624-1633.	3.0	89
294	Non-invasive study of human gall bladder bilein vivousing1H-MR spectroscopy. British Journal of Radiology, 2003, 76, 483-486.	1.0	5
295	Sliding window dual gradient echo (SW-dGRE):T1and proton resonance frequency (PRF) calibration for temperature imaging in polyacrylamide gel. Physics in Medicine and Biology, 2003, 48, 1917-1931.	1.6	8
296	Could assessment of glioma methylene lipid resonance byin vivo1H-MRS be of clinical value?. British Journal of Radiology, 2003, 76, 459-463.	1.0	44
297	Human Gallbladder Bile: Noninvasive Investigation in Vivo with Single-Voxel1H MR Spectroscopy. Radiology, 2003, 229, 587-592.	3.6	27
298	A phase I study of SR-4554 via intravenous administration for noninvasive investigation of tumor hypoxia by magnetic resonance spectroscopy in patients with malignancy. Clinical Cancer Research, 2003, 9, 5101-12.	3.2	40
299	Comparison of biomechanical breast models: a case study. , 2002, , .		24
300	Early <i>in vivo</i> detection of metabolic response: a pilot study of <sup>1</sup> H MR spectroscopy in extracranial lymphoma and germ cell tumours. British Journal of Radiology, 2002, 75, 959-966.	1.0	53
301	An algorithm for the optimum combination of data from arbitrary magnetic resonance phased array probes. Physics in Medicine and Biology, 2002, 47, N39-N46.	1.6	25
302	Comparison between radiological and artificial neural network diagnosis in clinical screening. Physiological Measurement, 2002, 23, 727-739.	1.2	21
303	A model to assess SAR for surface coil magnetic resonance spectroscopy measurements. Physics in Medicine and Biology, 2002, 47, 1805-1817.	1.6	4
304	Finite-element based validation of nonrigid registration using single- and multilevel free-form deformations: application to contrast-enhanced MR mammography. , 2002, 4684, 550.		4
305	Human rectal adenocarcinoma: Demonstration of1H-MR spectra in vivo at 1.5 T. Magnetic Resonance in Medicine, 2002, 47, 809-811.	1.9	32
306	Reproducibility of quantitative dynamic MRI of normal human tissues. NMR in Biomedicine, 2002, 15, 143-153.	1.6	183

#	Article	IF	CITATIONS
307	Applications of sliding window reconstruction with cartesian sampling for dynamic contrast enhanced MRI. NMR in Biomedicine, 2002, 15, 174-183.	1.6	68
308	Assessing changes in tumour vascular function using dynamic contrast-enhanced magnetic resonance imaging. NMR in Biomedicine, 2002, 15, 154-163.	1.6	250
309	The effect of Gd-DTPA on T1-weighted choline signal in human brain tumours. Magnetic Resonance Imaging, 2002, 20, 127-130.	1.0	34
310	What is the recall rate of breast MRI when used for screening asymptomatic women at high risk?. Magnetic Resonance Imaging, 2002, 20, 557-565.	1.0	19
311	Apoptosis is associated with triacylglycerol accumulation in Jurkat T-cells. British Journal of Cancer, 2002, 86, 963-970.	2.9	107
312	Validation of Volume-Preserving Non-rigid Registration: Application to Contrast-Enhanced MR-Mammography. Lecture Notes in Computer Science, 2002, , 307-314.	1.0	20
313	Validation of Non-rigid Registration of Contrast-Enhanced MR Mammography Using Finite Element Methods. Informatik Aktuell, 2002, , 143-146.	0.4	2
314	The effects of paramagnetic contrast agents on metabolite protons in aqueous solution. Physics in Medicine and Biology, 2002, 47, N53-9.	1.6	9
315	Assessing response to treatment in breast cancer using magnetic resonance. Journal of Experimental and Clinical Cancer Research, 2002, 21, 39-45.	0.4	0
316	The UK national study of magnetic resonance imaging as a method of screening for breast cancer (MARIBS). Journal of Experimental and Clinical Cancer Research, 2002, 21, 107-14.	0.4	7
317	Radio-frequency probe for 1H decoupled 31P MRS of the head and neck region. Magnetic Resonance Imaging, 2001, 19, 755-759.	1.0	17
318	The quantitative 19 F-imaging of albumin at 1.5 T: a potential in-vivo tool. Magnetic Resonance Imaging, 2001, 19, 839-844.	1.0	8
319	In vivo hyperpolarized129Xe NMR spectroscopy in tumors. Magnetic Resonance in Medicine, 2001, 46, 586-591.	1.9	27
320	Effects of Chronic Alcohol Consumption on the Broad Phospholipid Signal in Human Brain: An In Vivo 31P MRS Study. Alcoholism: Clinical and Experimental Research, 2001, 25, 89-97.	1.4	30
321	Effects of Abstinence From Alcohol on the Broad Phospholipid Signal in Human Brain: An In Vivo 31P Magnetic Resonance Spectroscopy Study. Alcoholism: Clinical and Experimental Research, 2001, 25, 1213-1220.	1.4	22
322	Magnetic resonance detects changes in phosphocholine associated with Ras activation and inhibition in NIH 3T3 cells. British Journal of Cancer, 2001, 84, 691-696.	2.9	68
323	Measuring changes in human tumour vasculature in response to therapy using functional imaging techniques. British Journal of Cancer, 2001, 85, 1085-1093.	2.9	63
324	Pre-processed image reconstruction applied to breast and brain MR imaging. Physiological Measurement, 2001, 22, 589-604.	1.2	2

#	Article	IF	CITATIONS
325	Effects of Androgen Deprivation on Prostatic Morphology and Vascular Permeability Evaluated with MR Imaging. Radiology, 2001, 218, 365-374.	3.6	143
326	Numerical evaluation of shaped surface coil sensitivity at 63 MHz. Physics in Medicine and Biology, 2001, 46, 1753-1765.	1.6	9
327	Validation of Non-rigid Registration Using Finite Element Methods. Lecture Notes in Computer Science, 2001, , 344-357.	1.0	34
328	Hyperpolarized129Xe NMR as a probe for blood oxygenation. Magnetic Resonance in Medicine, 2000, 43, 491-496.	1.9	98
329	Surface-coil polarization transfer for monitoring tissue metabolism in vivo. Magnetic Resonance in Medicine, 2000, 43, 510-516.	1.9	11
330	Proton magnetic resonance spectroscopy (1H-MRS) of the brain following high-dose methotrexate treatment for childhood cancer. Medical and Pediatric Oncology, 2000, 35, 28-34.	1.0	29
331	1H decoupling for in vivo19F MRS studies using the time-share modulation method on a clinical 1.5 T NMR system. Magnetic Resonance in Medicine, 2000, 44, 5-9.	1.9	9
332	Initial measurements of ifosfamide and cyclophosphamide in patients using31P MRS: Pulse-and-acquire, decoupling, and polarization transfer. Magnetic Resonance in Medicine, 2000, 44, 180-184.	1.9	13
333	Gallbladder localization of 19F MRS catabolite signals in patients receiving bolus and protracted venous infusional 5-fluorouracil. Magnetic Resonance in Medicine, 2000, 44, 516-520.	1.9	25
334	SAR and tissue heating with a clinical31P MRS protocol using surface coils, adiabatic pulses, and proton-decoupling. Magnetic Resonance in Medicine, 2000, 44, 692-700.	1.9	12
335	On the oxygenation-dependent129XeT1 in blood. NMR in Biomedicine, 2000, 13, 234-237.	1.6	32
336	Intravenous delivery of hyperpolarized129Xe: a compartmental model. NMR in Biomedicine, 2000, 13, 238-244.	1.6	24
337	High-resolution segmented EPI in a motor task fMRI study. Magnetic Resonance Imaging, 2000, 18, 405-409.	1.0	49
338	Magnetic resonance imaging screening in women at genetic risk of breast cancer: imaging and analysis protocol for the UK multicentre study. Magnetic Resonance Imaging, 2000, 18, 765-776.	1.0	104
339	Improving image quality and T1 measurements using saturation recovery turboFLASH with an approximate K-space normalisation filter. Magnetic Resonance Imaging, 2000, 18, 157-167.	1.0	40
340	Rationale for a national multi-centre study of magnetic resonance imaging screening in women at genetic risk of breast cancer. Breast, 2000, 9, 72-77.	0.9	24
341	Protocol for a national multi-centre study of magnetic resonance imaging screening in women at genetic risk of breast cancer. Breast, 2000, 9, 78-82.	0.9	22
342	Preclinical development of noninvasive vascular occlusion with focused ultrasonic surgery for fetal therapy. American Journal of Obstetrics and Gynecology, 2000, 182, 387-392.	0.7	41

#	Article	IF	CITATIONS
343	A modified polymer gel for radiotherapy dosimetry: assessment by MRI and MRS. Physics in Medicine and Biology, 2000, 45, 3213-3223.	1.6	25
344	Radiotherapy planning of the pelvis using distortion corrected MR images: the removal of system distortions. Physics in Medicine and Biology, 2000, 45, 2117-2132.	1.6	57
345	The reproducibility of polyacrylamide gel dosimetry applied to stereotactic conformal radiotherapy. Physics in Medicine and Biology, 2000, 45, 1195-1210.	1.6	57
346	Magnetic resonance spectroscopy in the evaluation of neurotoxicity following cranial irradiation for childhood cancer British Journal of Radiology, 2000, 73, 421-424.	1.0	34
347	Proton spectroscopic imaging of polyacrylamide gel dosimeters for absolute radiation dosimetry. Physics in Medicine and Biology, 2000, 45, 835-845.	1.6	32
348	Implications of respiratory motion for the quantification of 2D MR spectroscopic imaging data in the abdomen. Physics in Medicine and Biology, 2000, 45, 2105-2116.	1.6	43
349	Dynamic Contrast Enhanced MRI of Prostate Cancer: Correlation with Morphology and Tumour Stage, Histological Grade and PSA. Clinical Radiology, 2000, 55, 99-109.	0.5	320
350	Optimized MR imaging for polyacrylamide gel dosimetry. Physics in Medicine and Biology, 2000, 45, 847-858.	1.6	37
351	Imaging biochemistry: applications to breast cancer. Breast Cancer Research, 2000, 3, 36-40.	2.2	55
352	Breast imaging technology Application of magnetic resonance imaging to angiogenesis in breast cancer. Breast Cancer Research, 2000, 3, 22-7.	2.2	57
353	Radiation dosimetry using polymer gels: methods and applications British Journal of Radiology, 2000, 73, 919-929.	1.0	118
354	Dynamics of polymerization in polyacrylamide gel (PAC) dosimeters: (II) modelling oxygen diffusion. Physics in Medicine and Biology, 1999, 44, 1875-1884.	1.6	72
355	Comparison of MRI with CT for the radiotherapy planning of prostate cancer: a feasibility study British Journal of Radiology, 1999, 72, 590-597.	1.0	81
356	Spin-lattice relaxation of laser-polarized xenon in human blood. Proceedings of the National Academy of Sciences of the United States of America, 1999, 96, 3664-3669.	3.3	64
357	Vascular occlusion using focused ultrasound surgery for use in fetal medicine. European Journal of Ultrasound: Official Journal of the European Federation of Societies for Ultrasound in Medicine and Biology, 1999, 9, 89-97.	1.4	51
358	Evaluating the effect of rectal distension and rectal movement on prostate gland position using cine MRI. International Journal of Radiation Oncology Biology Physics, 1999, 44, 525-533.	0.4	262
359	Magnetic resonance detects metabolic changes associated with chemotherapy-induced apoptosis. British Journal of Cancer, 1999, 80, 1035-1041.	2.9	50
360	Dynamics of polymerization in polyacrylamide gel (PAG) dosimeters: (I) ageing and long-term stability. Physics in Medicine and Biology, 1999, 44, 1863-1873.	1.6	62

#	Article	IF	CITATIONS
361	Dynamic contrast-enhanced MRI in the differentiation of breast tumors: User-defined versus semi-automated region-of-interest analysis. Journal of Magnetic Resonance Imaging, 1999, 10, 945-949.	1.9	76
362	Perfluorocarbon emulsions as intravenous delivery media for hyperpolarized xenon. Magnetic Resonance in Medicine, 1999, 41, 442-449.	1.9	63
363	Signal modulation in1H magnetic resonance spectroscopy using contrast agents: Proton relaxivities of choline, creatine, andN-acetylaspartate. Magnetic Resonance in Medicine, 1999, 42, 1155-1158.	1.9	25
364	Measurement of the extracellular pH of solid tumours in mice by magnetic resonance spectroscopy: a comparison of exogenous19F and31P probes. NMR in Biomedicine, 1999, 12, 495-504.	1.6	206
365	Experimental 3D dosimetry around a high-dose-rate clinical192Ir source using a polyacrylamide gel (PAG) dosimeter. Physics in Medicine and Biology, 1999, 44, 2431-2444.	1.6	56
366	Nonrigid registration using free-form deformations: application to breast MR images. IEEE Transactions on Medical Imaging, 1999, 18, 712-721.	5.4	4,317
367	<title>Comparison and evaluation of rigid and nonrigid registration of breast MR images</title> . , 1999, 3661, 78.		19
368	Comparison and Evaluation of Rigid, Affine, and Nonrigid Registration of Breast MR Images. Journal of Computer Assisted Tomography, 1999, 23, 800-805.	0.5	103
369	Measuring diffusion of xenon in solution with hyperpolarized 129Xe NMR. Chemical Physics Letters, 1998, 296, 391-396.	1.2	35
370	In VivoMultiple Spin Echoes. Journal of Magnetic Resonance, 1998, 135, 30-36.	1.2	41
371	Measurements of human breast cancer using magnetic resonance spectroscopy: a review of clinical measurements and a report of localized31P measurements of response to treatment. , 1998, 11, 314-340.		125
372	Intravascular delivery of hyperpolarized129Xenon forin vivo MRI. Applied Magnetic Resonance, 1998, 15, 343-352.	0.6	11
373	A Simple Phantom to Locate the Origin of MRI Ghost Artefacts. Magnetic Resonance Imaging, 1998, 16, 73-76.	1.0	0
374	Absolute metabolite quantification by in vivo NMR spectroscopy: I. introduction, objectives and activities of a concerted action in biomedical research. Magnetic Resonance Imaging, 1998, 16, 1085-1092.	1.0	21
375	Absolute metabolite quantification by in vivo NMR spectroscopy: II. a multicentre trial of protocols for in vivo localised proton studies of human brain. Magnetic Resonance Imaging, 1998, 16, 1093-1106.	1.0	98
376	An investigation into the dosimetry of a nine-field tomotherapy irradiation using BANG-gel dosimetry. Physics in Medicine and Biology, 1998, 43, 1113-1132.	1.6	124
377	MRIW: parametric analysis software for contrast-enhanced dynamic MR imaging in cancer Radiographics, 1998, 18, 497-506.	1.4	55
378	Improving calibration accuracy in gel dosimetry. Physics in Medicine and Biology, 1998, 43, 2709-2720.	1.6	101

#	Article	IF	CITATIONS
379	Influence of pH on the uptake of 5-fluorouracil into isolated tumour cells. British Journal of Cancer, 1998, 77, 873-879.	2.9	48
380	<title>Focused ultrasound surgery-induced vascular occlusion in fetal medicine</title> . , 1998, , .		4
381	Carbogen breathing increases 5-fluorouracil uptake and cytotoxicity in hypoxic murine RIF-1 tumors: a magnetic resonance study in vivo. Cancer Research, 1998, 58, 1185-94.	0.4	46
382	Quantification of phosphorus metabolites in human calf muscle and soft-tissue tumours from localized MR spectra acquired using surface coils. Physics in Medicine and Biology, 1997, 42, 691-706.	1.6	16
383	MRI study of hepatic tumours following high intensity focused ultrasound surgery British Journal of Radiology, 1997, 70, 144-153.	1.0	86
384	<title>Visual detectability of elastic contrast in real-time ultrasound images</title> . , 1997, , .		2
385	Magnetic resonance imaging (MRI): considerations and applications in radiotherapy treatment planning. Radiotherapy and Oncology, 1997, 42, 1-15.	0.3	266
386	A pharmacokinetic and pharmacodynamic study In vivo of human HT29 tumours using 19F and 31P magnetic resonance spectroscopy. European Journal of Cancer, 1997, 33, 2418-2427.	1.3	31
387	Probing tumor microvascularity by measurement, analysis and display of contrast agent uptake kinetics. Journal of Magnetic Resonance Imaging, 1997, 7, 564-574.	1.9	191
388	Implementation and evaluation of frequency offset corrected inversion (FOCI) pulses on a clinical MR system. Magnetic Resonance in Medicine, 1997, 38, 828-833.	1.9	35
389	Simultaneous localized <sup>1</sup> H STEAM/ <sup>31</sup> P ISIS spectroscopy <i>in Vivo</i> . Magnetic Resonance in Medicine, 1996, 35, 465-470.	1.9	8
390	Measurement of plasma 5-fluorouracil by high-performance liquid chromatography with comparison of results to tissue drug levels observed using in vivo 19F magnetic resonance spectroscopy in patients on a protracted venous infusion with or without interferon-α. Annals of Oncology, 1996, 7, 47-53.	0.6	56
391	MRI in the evaluation of late bone marrow changes following bone marrow transplantation. British Journal of Radiology, 1996, 69, 1145-1151.	1.0	12
392	Phosphocholine and choline content of rat sarcoma cells grown in the presence and absence of serum. Anticancer Research, 1996, 16, 1389-92.	0.5	5
393	Introduction to in vivo MRS of cancer: new perspectives and open problems. Anticancer Research, 1996, 16, 1503-14.	0.5	19
394	Calculation of Sensitivity Correction Factors for Surface Coil MRS. Magnetic Resonance in Medicine, 1995, 33, 108-112.	1.9	13
395	Pharmacokinetics of the13C labeled anticancer agent temozolomide detectedin vivo by selective cross-polarization transfer. Magnetic Resonance in Medicine, 1995, 34, 338-342.	1.9	28
396	Increased noe enhancement in1h decoupled31p mrs. Magnetic Resonance in Medicine, 1995, 34, 893-897.	1.9	7

#	Article	IF	CITATIONS
397	Quality assessment in in vivo NMR spectroscopy: II. A protocol for quality assessment. Magnetic Resonance Imaging, 1995, 13, 123-129.	1.0	34
398	Quality assessment in in vivo NMR spectroscopy: III. Clinical test objects: Design, construction, and solutions. Magnetic Resonance Imaging, 1995, 13, 131-137.	1.0	45
399	Quality assessment in in vivo NMR spectroscopy: IV. A multicentre trial of test objects and protocols for performance assessment in clinical NMR spectroscopy. Magnetic Resonance Imaging, 1995, 13, 139-157.	1.0	41
400	On doubling the signal in localised stimulated echo measurements. Magnetic Resonance Imaging, 1995, 13, 629-632.	1.0	4
401	Quantification of signal selection efficiency, extra volume suppression and contamination for ISIS, STEAM and PRESS localized1H NMR spectroscopy using an EEC localization test object. Physics in Medicine and Biology, 1995, 40, 1293-1303.	1.6	24
402	Reducing motion artifacts in <i>in vivo</i> magnetic resonance imaging measurements of relaxation times. British Journal of Radiology, 1994, 67, 1249-1257.	1.0	0
403	A gradient scheme suitable for localized shimming andin vivo1H/31P STEAM and ISIS NMR spectroscopy. Magnetic Resonance in Medicine, 1994, 32, 768-772.	1.9	4
404	In vivo monitoring of fluoropyrimidine metabolites. Anti-Cancer Drugs, 1994, 5, 260-280.	0.7	28
405	The effect of oestrogen ablation on the phospholipid metabolite content of primary and transplanted rat mammary tumours. NMR in Biomedicine, 1993, 6, 209-214.	1.6	7
406	Phospholipid metabolites, prognosis and proliferation in human breast carcinoma. NMR in Biomedicine, 1993, 6, 318-323.	1.6	43
407	A rapid interleaved method for measuring signal intensity curves in both blood and tissue during contrast agent administration. Magnetic Resonance in Medicine, 1993, 30, 744-749.	1.9	18
408	The non-invasive monitoring of low dose, infusional 5-fluorouracil and its modulation by interferon-α using in vivo 19F magnetic resonance spectroscopy in patients with colorectal cancer: A pilot study. Annals of Oncology, 1993, 4, 597-602.	0.6	60
409	Magnetic resonance imaging and spectroscopy: An introduction to theory, hardware, current applications and safety. Journal of Radiological Protection, 1992, 12, 137-158.	0.6	1
410	A single-shot shimming sequence using low-power RF noise pulses for localized in vivo NMR spectroscopy. Physics in Medicine and Biology, 1992, 37, 281-287.	1.6	6
411	Radial diffusion coefficient mapping. British Journal of Radiology, 1992, 65, 885-894.	1.0	0
412	Quantitative magnetic resonance spectroscopy by optimized numerical curve fitting. NMR in Biomedicine, 1992, 5, 87-94.	1.6	5
413	A two-point volume localized T1 measurement sequence forin vivo spectroscopy using a surface coil. NMR in Biomedicine, 1992, 5, 95-100.	1.6	6
414	Threshold voltages for hyperbolic secant inversion pulses. NMR in Biomedicine, 1992, 5, 142-144.	1.6	5

#	Article	IF	CITATIONS
415	Practicalities of localization in animal and human tumours. NMR in Biomedicine, 1992, 5, 244-252.	1.6	4
416	Rapid localization of concave volumes by conformal NMR spectroscopy. Magnetic Resonance in Medicine, 1992, 23, 386-393.	1.9	2
417	Fast and accurate measurements of T1 using a multi-readout single inversion-recovery sequence. Magnetic Resonance in Medicine, 1992, 26, 79-88.	1.9	40
418	Clinical 19F Nuclear Magnetic Resonance Spectroscopy in Colorectal Cancer: Monitoring Low-Level 5-Fluorouracil Infusion Therapy and the Metabolic Effects of Additive α-Interferon. , 1992, , 213-218.		0
419	A phase II clinical and pharmacokinetic study of Lonidamine in patients with advanced breast cancer. British Journal of Cancer, 1991, 64, 593-597.	2.9	34
420	A comparison of in vivo and in vitro 31P NMR spectra from human breast tumours: variations in phospholipid metabolism. British Journal of Cancer, 1991, 63, 514-516.	2.9	60
421	The phosphocholine and glycerophosphocholine content of an oestrogen-sensitive rat mammary tumour correlates strongly with growth rate. British Journal of Cancer, 1991, 64, 821-826.	2.9	71
422	A quantitative analysis of the accuracy ofIn Vivo pH measurements with31P NMR spectroscopy: Assessment of pH measurement methodology. NMR in Biomedicine, 1991, 4, 1-11.	1.6	47
423	The effect of intra-tumour heterogeneity on the distribution of phosphorus-containing metabolites within human breast tumours: AnIn Vitro study using31P NMR spectroscopy. NMR in Biomedicine, 1991, 4, 262-267.	1.6	31
424	A simple method for the restoration of signal polarity in multi-image inversion recovery sequences for measuring T1. Magnetic Resonance in Medicine, 1991, 18, 224-231.	1.9	39
425	The water resonance as an alternative pH reference: Relevance toin Vivo31P NMR localized spectroscopy studies. Magnetic Resonance in Medicine, 1991, 19, 416-421.	1.9	17
426	Comparison of 5-Fluorouracil pharmacokinetics following intraperitoneal and intravenous administration using <i>in vivo</i> Â19F magnetic resonance spectroscopy. British Journal of Radiology, 1990, 63, 547-553.	1.0	34
427	An assessment of the sensitivity of <i>in vivo</i> Â31P nuclear magnetic resonance spectroscopy as a means of detecting pH heterogeneity in tumours: a simulation study. British Journal of Radiology, 1990, 63, 120-124.	1.0	10
428	Improving the Accuracy of T1 Measurements In Vivo: The Use of the Hyperbolic Secant Pulse in the Saturation Recovery/Inversion Recovery Sequence. , 1990, , 36-42.		1
429	Installation of an ambient-temperature control system in a 1.5-tesla whole body system to facilitate animal studies. Medical Physics, 1989, 16, 916-919.	1.6	0
430	pH calibration curve at 1.5 Tesla. Physics in Medicine and Biology, 1989, 34, 1289-1293.	1.6	4
431	Conformal NMR spectroscopy: Accurate localization to noncuboidal volumes with optimum SNR. Magnetic Resonance in Medicine, 1989, 11, 376-388.	1.9	23
432	The use of an improved inversion pulse with the Spin-Echo/ inversion-recovery sequence to give increased accuracy and reduced imaging time for T1 measurements. Magnetic Resonance in Medicine, 1989, 12, 261-267.	1.9	23

#	Article	IF	CITATIONS
433	IN-VIVO 31P MAGNETIC RESONANCE SPECTROSCOPY FOR MONITORING TREATMENT RESPONSE IN BREAST CANCER. Lancet, The, 1989, 333, 1326-1327.	6.3	68
434	The performance characteristics of a simulator-based CT scanner. IEEE Transactions on Medical Imaging, 1988, 7, 91-98.	5.4	4
435	Clinical dosimetry for radiotherapy to the breast based on imaging with the prototype Royal Marsden Hospital CT simulator. Physics in Medicine and Biology, 1987, 32, 835-845.	1.6	39
436	Measurement of radiation dose to the thyroid using positron emission tomography. British Journal of Radiology, 1987, 60, 245-251.	1.0	43
437	3D positron emission tomography: preliminary results. British Journal of Radiology, 1986, 59, 419-422.	1.0	6
438	The design and use of a dual-frequency surface coil providing proton images for improved localization in 3 1 P spectroscopy of small lesions. Medical Physics, 1986, 13, 510-513.	1.6	16
439	The development of high-efficiency cathode converters for a multiwire proportional chamber positron camera. Medical Physics, 1986, 13, 703-706.	1.6	12
440	An X-ray detector system and modified simulator providing CT images for radiotherapy dosimetry planning. Physics in Medicine and Biology, 1985, 30, 303-311.	1.6	8
441	Constrained deconvolution of SPECT liver tomograms by direct digital image restoration. Medical Physics, 1985, 12, 53-58.	1.6	48
442	The measurement of resolution in single photon emission computerised tomography. Physics in Medicine and Biology, 1984, 29, 282-283.	1.6	2
443	The release rate of37Ar from human subjects following intravenous injection. Physics in Medicine and Biology, 1984, 29, 779-788.	1.6	1
444	Reconstructions from a Nonstandard CT Scanner. IEEE Transactions on Medical Imaging, 1984, 3, 193-196.	5.4	7
445	A clinical evaluation of a prototype positron camera for longitudinal emission tomography. British Journal of Radiology, 1984, 57, 1103-1117.	1.0	8
446	The Application of Variable Median Window Filtering to Computerised Tomography. , 1984, , 151-168.		3
447	A comparison of attenuation correction methods for quantitative single photon emission computed tomography. Physics in Medicine and Biology, 1983, 28, 1045-1056.	1.6	22
448	The retention and release of37Ar from samples of human bone examined in vitro and a review of the implications for argon transfer from bone in vivo. Physics in Medicine and Biology, 1983, 28, 389-405.	1.6	3
449	Preliminary clinical images from a prototype positron camera. British Journal of Radiology, 1983, 56, 773-776.	1.0	8
450	A comparison between 180° and 360° data reconstruction in single photon emission computed tomography of the liver and spleen. British Journal of Radiology, 1983, 56, 931-937.	1.0	7

1

#	Article	IF	CITATIONS
451	The spatial resolution of a rotating gamma camera tomographic facility. British Journal of Radiology, 1983, 56, 939-944.	1.0	10
452	A rotate-translate CT scanner providing cross-sectional data suitable for planning the dosimetry of radiotherapy treatment. Medical Physics, 1982, 9, 269-275.	1.6	6
453	Blood flow measurements and the partition coefficient of133Xe in bone. Physics in Medicine and Biology, 1982, 27, 1401-1403.	1.6	2
454	A compartmental model for investigating the influence of physiological factors on the rate of washout of133Xe and37Ar from the body. Physics in Medicine and Biology, 1982, 27, 1105-1118.	1.6	8
455	The preparation of 37Ar in sterile solution suitable for injection in vivo. The International Journal of Applied Radiation and Isotopes, 1982, 33, 586-588.	0.7	2
456	In vivo measurement of calcium by the 37Ar method: a study of the effect of recirculating breath collection systems on the exhalation rate. Physics in Medicine and Biology, 1978, 23, 282-290.	1.6	7
457	Problems in the interpretation of the in vivo measurement of calcium by the argon-37 method: an investigation of inert-gas elimination in humans. Journal of Nuclear Medicine, 1978, 19, 54-60.	2.8	9
458	Total body nitrogen measured by the method: A study of the interfering reactions and the variation of spatial sensitivity with depth. The International Journal of Applied Radiation and Isotopes, 1977, 28, 263-269.	0.7	17
459	Metabolomic Magnetic Resonance Spectroscopy of Human Tissues: Comparison of In Vivo and High-Resolution Magic Angle Spinning Ex Vivo Techniques. , 0, , 472-495.		0

460 Content Based Image Retrieval for Dynamic Time Series Data. , 0, , 61-65.